

Ion neutralization and high-energy electron emission in He⁺ scattering by a highly oriented pyrolytic graphite surface

A. Iglesias-García,¹ F. Bonetto,^{1,2} R. Vidal,^{1,2} J. Ferrón,^{1,2} and E. C. Goldberg^{1,2}

¹*Instituto de Física del Litoral (CONICET-UNL), Guemes 3450, Santa Fé, Argentina*

²*Facultad de Ingeniería Química, Universidad Nacional del Litoral, Santiago del Estero 2829, Santa Fé, Argentina*

(Received 26 December 2013; published 3 April 2014)

We report results of ion neutralization of low-energy positive He ions interacting with a surface of highly oriented pyrolytic graphite as a function of the impinging energy. We found a neutralization probability close to unity for a wide energy range. This behavior is reproduced by our theory only if we take into account the electronic correlation introduced by the He first excited states considered as possible neutralization channels. The finite occupation of these excited states opens the Auger deexcitation process as a source of emitted electrons. The calculation of this electron emitted spectrum is complex as it requires the knowledge of the energies and occupations of the atomic configurations as a function of the ion trajectory. Our calculation shows the presence of high energetic secondary electrons contributing to the Auger electron emission spectra of this system [N. Bajales, L. Cristina, S. Mendoza, R. A. Baragiola, E. C. Goldberg, and J. Ferrón, *Phys. Rev. Lett.* **100**, 227604 (2008)].

DOI: [10.1103/PhysRevA.89.042702](https://doi.org/10.1103/PhysRevA.89.042702)

PACS number(s): 79.20.Rf, 34.70.+e, 68.49.Sf

I. INTRODUCTION

The final charge states of ions scattered by a surface as well as the associated electron emission provide abundant information about the details of the surface electronic band structure and the interacting atoms' correlated states [1–14]. This fact has motivated the development of new theoretical proposals that, following feedback with experimental data, allow for a deep understanding of the underlying physical mechanisms.

The high neutralization of helium positive ions colliding with a highly oriented pyrolytic graphite (HOPG) surface has been extensively discussed from a theoretical point of view in a previous work [15]. It was found that the correlation between the ground state He ($1s^2$) and the excited states, ($1s2s$) and ($1s2p$), through their interaction with the surface band states, notably strengthens the neutralization to the ground state. Furthermore, Auger deexcitation, following neutralization to the excited states, additionally contributes to the total neutral fraction of He atoms in the ground state [1,16–19]. There is plenty of experimental evidence [20–23] showing a practically full neutralization of He⁺ projectiles scattered off a HOPG surface. However, a systematic and direct measurement of the energy dependence of neutralization with its corresponding comparison with theoretical results [15] is still lacking. In addition, the large reported experimental errors so far have not allowed for the detection of potential slight dependences of the neutralization with the energy. Simultaneously, the He ions colliding with the HOPG surface, at different energies, induce the emission of high-energy electrons (up to 35–40 eV) whose origin is not completely understood [24,25].

In this work, we present experimental results of neutral fractions of He⁺ impinging on a HOPG surface obtained by using the low-energy ion scattering spectrometry technique with time-of-flight analysis (LEIS-TOF) [26]. Our measurements were performed in a backscattering configuration (135° scattering and 90° exit angle) in the 1–8 keV energy range with 1 keV step. In all cases, neutral fractions were obtained with

a relative error lower than 2%, being higher at lower energies. A slight but still detectable dependence with the energy was found. The theoretical neutral fractions show a satisfactory agreement with the experimental results only when excited He states are included as possible neutralization channels [15]. In this way, the idea of an Auger deexcitation process as an alternative source of electron emission is reinforced. The variation along the ion trajectory of the energies of the active atomic configurations and their occupation probabilities allow for a calculation of the secondary electron spectra within a semiclassical approximation of the Auger decaying process.

This work is organized as follows: in Sec. II, we present a brief discussion of the theoretical calculation of the neutral fraction since a more exhaustive discussion can be found in Ref. [15]; in Sec. III, we depict the experimental details of the neutral fraction measurement, and a comparison between both, theory and experiment, is performed in Sec. IV. The calculation of the emitted electron spectra and comparison with experimental results are discussed in Sec. V. Finally, the concluding remarks are presented in Sec. VI.

II. THEORETICAL CALCULATION OF THE NEUTRAL FRACTION

The He ion neutralization model we are testing here has been fully developed in a previous work [15]. Since an extension of the model is necessary to study electron emission, in the following we offer a summary of the theoretical framework employed.

We perform a quantum-mechanical calculation that includes the resonant neutralization to the ground state and to the first excited He ion states. We start with the extended Anderson's Hamiltonian [27],

$$\hat{H} = \sum_{\vec{k},\sigma} \varepsilon_{\vec{k}} \hat{n}_{\vec{k}\sigma} + \hat{H}_{\text{ion}} + \sum_{\vec{k}m,\sigma} (\hat{V}_{\vec{k}m}^{\sigma} \hat{c}_{\vec{k}\sigma}^{\dagger} \hat{c}_{m\sigma} + \text{H.c.}) + [\text{Auger terms}], \quad (1)$$

where $\hat{c}_{\vec{k}\sigma}^+$ and $\hat{c}_{m\sigma}^+$ denote the creation operators of the conduction electron and the localized electrons in the atomic orbitals m with spin σ , $\hat{n}_{\vec{k}\sigma}$ is the occupation number operator for the band states, and \hat{V}_{km}^σ are the couplings between the conduction and localized electrons in the atomic orbital m . \hat{H}_{ion} corresponds to the atomic system including the one- and two-electron interactions between the different orbitals, defined as

$$\begin{aligned} \hat{H}_{\text{ion}} = & \sum_{m,\sigma} \zeta_m \hat{n}_{m\sigma} + \sum_m U_m \hat{n}_{m\uparrow} \hat{n}_{m\downarrow} \\ & + \frac{1}{2} \sum_{m \neq m', \sigma} J_{mm'} \hat{n}_{m\sigma} \hat{n}_{m'-\sigma} \\ & + \frac{1}{2} \sum_{m \neq m', \sigma} (J_{mm'} - J_{mm'}^x) \hat{n}_{m\sigma} \hat{n}_{m'\sigma} \\ & - \frac{1}{2} \sum_{m \neq m', \sigma} J_{mm'}^x \hat{c}_{m\sigma}^+ \hat{c}_{m-\sigma} \hat{c}_{m'-\sigma}^+ \hat{c}_{m'\sigma}, \end{aligned} \quad (2)$$

where U and J are the direct Coulomb intra-atomic interactions, while J^x is the exchange one. The first term is related to the kinetic energy and electron-nuclei potential, and the fifth term, related to spin-flip processes, restores the invariance under rotation in spin space. The atomic part of the Hamiltonian, considering many states in the ion projectile, requires applying the configuration interaction method within the time-dependent collision process, which is easily achieved in this work by using the projection operator approach.

After an analysis of the energy levels of the He atom interacting with the HOPG surface as a function of ion-surface distance [15], we found that the atomic configurations that can be probable neutralization channels of He⁺ ($1s$) are the ground-state $|1s\uparrow 1s\downarrow\rangle$ and the excited configurations $|1s\sigma 2\alpha\sigma\rangle$ and $|1s\sigma 2\alpha\bar{\sigma}\rangle$, corresponding to a total spin component S_z equal to 0 and 1, respectively ($\alpha = s, p_z$). By projecting the Anderson's Hamiltonian into these configurations, we obtain [15]

$$\begin{aligned} \hat{H}_{\text{ion}} = & E(1s\uparrow) \sum_{\sigma} |1s\sigma\rangle \langle 1s\sigma| \\ & + E(1s\uparrow 1s\downarrow) |1s\uparrow 1s\downarrow\rangle \langle 1s\uparrow 1s\downarrow| \\ & + \sum_{\sigma, \alpha=s, p} E(1s\uparrow 2\alpha\uparrow) |1s\sigma 2\alpha\sigma\rangle \langle 1s\sigma 2\alpha\sigma| \\ & + \sum_{\sigma, \alpha=s, p} E(1s\uparrow 2\alpha\downarrow) |1s\sigma 2\alpha\bar{\sigma}\rangle \langle 1s\sigma 2\alpha\bar{\sigma}|. \end{aligned} \quad (3)$$

The Auger terms in Eq. (1) are, in principle, related to Auger ground-state neutralization and to the Auger deexcitation of the populated He excited states. The first one can be neglected in this case because of the more efficient resonant mechanism occurring due to the energy position of the projectile level within the surface valence band. The Auger deexcitation process is assumed to start when the occupation of the excited states by the resonant mechanism has practically occurred [16]. In this form, the energy distribution of the Auger emitted electrons is calculated in a second step by using a semiclassical approximation, as described in Sec. V.

The interaction term in Eq. (1) related only to tunneling processes is projected into the selected atomic configurations, thus leading to the expression

$$\begin{aligned} \hat{H}_{\text{int}} = & \sum_{\vec{k}} [\tilde{V}_{\vec{k}1s} \hat{c}_{\vec{k}\uparrow}^+ |1s\downarrow\rangle \langle 1s\uparrow 1s\downarrow| + \text{H.c.}] \\ & - \sum_{\vec{k}} [\tilde{V}_{\vec{k}1s} \hat{c}_{\vec{k}\downarrow}^+ |1s\uparrow\rangle \langle 1s\uparrow 1s\downarrow| + \text{H.c.}] \\ & - \sum_{\vec{k}, \sigma, \alpha=s, p} [\tilde{V}_{\vec{k}2\alpha} \hat{c}_{\vec{k}\sigma}^+ |1s\sigma\rangle \langle 1s\sigma 2\alpha\sigma| + \text{H.c.}] \\ & - \sum_{\vec{k}, \sigma, \alpha=s, p} [\tilde{V}_{\vec{k}2\alpha} \hat{c}_{\vec{k}\bar{\sigma}}^+ |1s\sigma\rangle \langle 1s\sigma 2\alpha\bar{\sigma}| + \text{H.c.}]. \end{aligned} \quad (4)$$

In Eq. (3), $E(\cdot)$ represents the total energy of each atomic configuration; in Eq. (4), $\tilde{V}_{\vec{k}1s} = V_{\vec{k}1s}/\sqrt{N}$ and N accounts for the spin degeneration $N = 2$. The first two terms in Eq. (4) account for the spin statistic in the interaction of the ground state of the He atom with the surface states; the remaining terms describe the interaction of the atom excited configurations with the band states.

The physical quantities of interest are the occurrence probabilities of the different atomic configurations: the ion survival probability is given by $n_{He^+} = \sum_{\sigma} \langle |1s\sigma\rangle \langle 1s\sigma| \rangle$, the probability of neutralization to the ground state is $n_{He^0} = \langle |1s\uparrow 1s\downarrow\rangle \langle 1s\uparrow 1s\downarrow| \rangle$, the probability of neutralization to the excited states ($\alpha = s, p_z$) with $S_z = 1, -1$, $n_{He^0(1s2\alpha, S_z=1, -1)} = \sum_{\sigma} \langle |1s\sigma 2\alpha\sigma\rangle \langle 1s\sigma 2\alpha\sigma| \rangle$, and the probability of neutralization to the excited states with $S_z = 0$, $n_{He^0(1s2\alpha, S_z=0)} = \sum_{\sigma} \langle |1s\sigma 2\alpha\bar{\sigma}\rangle \langle 1s\sigma 2\alpha\bar{\sigma}| \rangle$. The time evolution of the occupation probabilities is calculated by using the equation of motion method (atomic units are used),

$$d\hat{n}/dt = -i[\hat{n}, \hat{H}];$$

by considering the energy degeneration and the normalization of the selected space of configurations, $n_{He^+} + n_{He^0} + \sum_{\alpha=s, p} [n_{He^0(1s2\alpha, S_z=1, -1)} + n_{He^0(1s2\alpha, S_z=0)}] = 1$, it is only necessary to calculate the motion equations of $\langle |1s\uparrow 1s\downarrow\rangle \langle 1s\uparrow 1s\downarrow| \rangle$, $\langle |1s\uparrow 2\alpha\uparrow\rangle \langle 1s\uparrow 2\alpha\uparrow| \rangle$, and $\langle |1s\uparrow 2\alpha\downarrow\rangle \langle 1s\uparrow 2\alpha\downarrow| \rangle$.

The atomic basis for the C and He atoms was taken from Ref. [28]. The $2s$ and $2p$ Gaussian orbitals used for the He atom [29] provide a good approximation of the energy of the first excited state 3S of He (19.73 eV against the experimental value of 19.82 eV) and also to the energy of the excited state 3P (20.5 eV compared with the experimental value 20.96 eV) [30].

The kinetic-energy loss of helium ions according to the experimental geometry (scattering angle of 135°) is taken into account, $E_{\text{out}} = 0.305 E_{\text{in}}$, with $E_{\text{in(out)}}$ the incoming (exit) kinetic energy of the projectile ion. In the calculation, the He atom moves perpendicular to the surface with a constant velocity $v_{\text{in(out)}}$, along a trajectory described by $z = z_{\text{rtp}} + v_{\text{in(out)}}|t|$, with z_{rtp} being the distance of closest approach to the surface, obtained from the He-C interaction energy. The $v_{\text{in(out)}}$ are the normal components of the ion velocity along the incoming (exit) trajectory, in accordance with the experimental setup. More details can be found in Ref. [15].

III. EXPERIMENT

Neutralization experiments were performed in the LEIS-TOF system available in our laboratory. Briefly, it consists of (1) an ultrahigh vacuum (UHV) chamber with a base pressure in the 10^{-9} Torr range; (2) an ion gun, that includes a Colutron ion source, focusing lens, a Wien filter, and pulsing plates; and (3) a time-of-flight (TOF) spectrometer.

The positive helium ions were produced in a discharge source (Colutron). After they are accelerated to the desired energy, a Wien filter is used to separate He^+ from other types of ions. In order to perform TOF measurements, a pulsed ion beam is produced by applying a square-wave voltage to a pair of deflection plates located in front of a rectangular slit. The pulsed ion beam, of about 1 mm in diameter, collides then with the HOPG substrate.

The HOPG sample was cleaved in air and cleaned in UHV by annealing at 1300 K for several minutes. During the whole experiment, the HOPG sample was kept at around 500 K to prevent potential contamination with implanted ions. After each set of experiments, the annealing process was repeated.

The scattered projectiles were detected by a channeltron electron multiplier (CEM) placed at the end of the drift tube (sample-detector distance: 137 cm). Deflection plates mounted at the TOF tube entrance allowed us to separate ions from neutral particles.

The ingoing and exit angles were selected to be 45° and 90° , measured with respect to the HOPG surface plane (total scattering angle: 135° ; see Fig. 1). This geometry was

particularly chosen to ensure consistency with the theoretical model assumptions and constraints.

TOF spectra for total (neutrals plus ions) and only neutral particles were recorded using a multiple-stop time spectrometer (Ortec MCS-plus). The elastic peak can be straightforwardly determined from the TOF spectra. To obtain the neutralization probability of ions scattered elastically from the HOPG surface, we select a narrow TOF interval of 200 ns (ΔE from 11 to 250 eV for incoming energies ranging from 1 to 8 keV, respectively) around the elastic peak. In order to increase the precision of our results, five sets (20 spectra each) of independent measurements were performed. Experimental errors were calculated from the statistical error of the complete set of measurements. In Fig. 1, we show a summary of the experimental results. The neutral fractions are close to unity, showing a slight decrease at the lowest and highest energies of the experimental range. These results are in agreement with those reported in Ref. [21] where the ion fractions were indirectly determined from LEIS using an electrostatic analyzer. In this work, the ion fractions were reported to be lower than 0.003 in the 1 to 3.5 keV range. In Ref. [22], it was reported that 500 eV incoming He^+ ions, at nearly normal incidence, are very efficiently neutralized after being scattered by a HOPG surface. In Ref. [23], a total neutralization was reported for 4 keV incoming ions backscattered using a specular geometric configuration. Therefore, we are reporting a direct and systematic measurement of the neutralization dependence with the incoming energy of He^+ ions backscattered by an

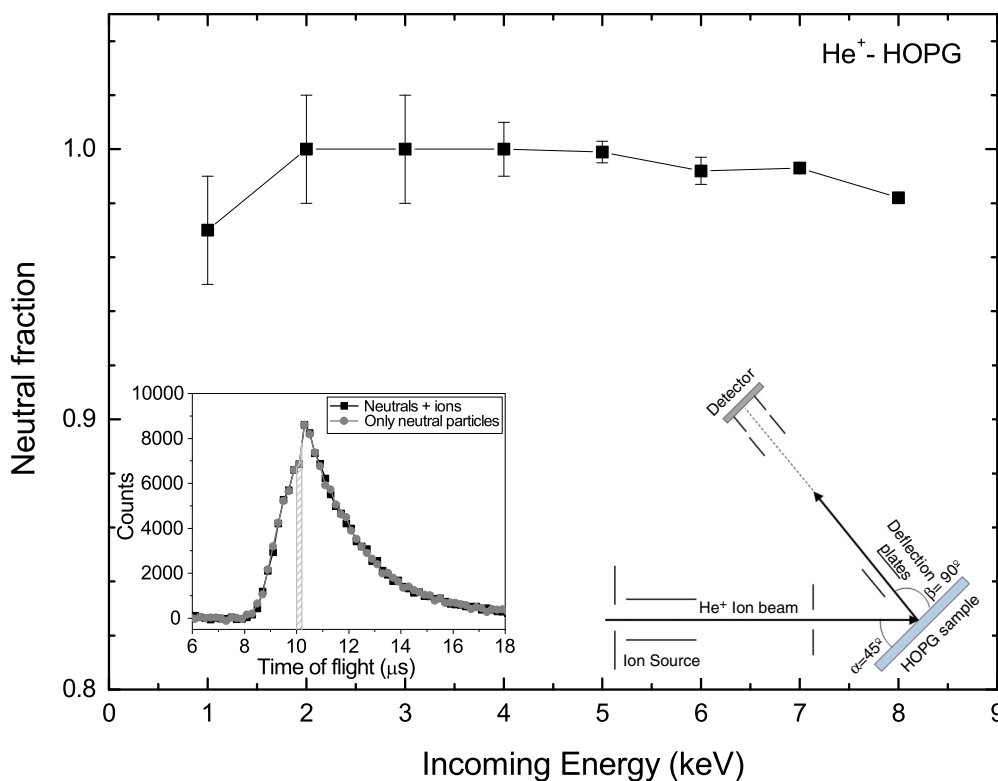


FIG. 1. Experimental He^+ -HOPG neutral fraction energy dependence. An almost complete neutralization is obtained except for slight departures at low and high incoming energies. TOF-LEIS spectra of total scattered (full squares, black) and neutral (full circles, gray) particles are shown for 2 keV projectile incoming energy (inset, left). The striped area specifies the elastic peak width considered for the neutral fraction calculation. The experimental geometry is shown in the right inset.

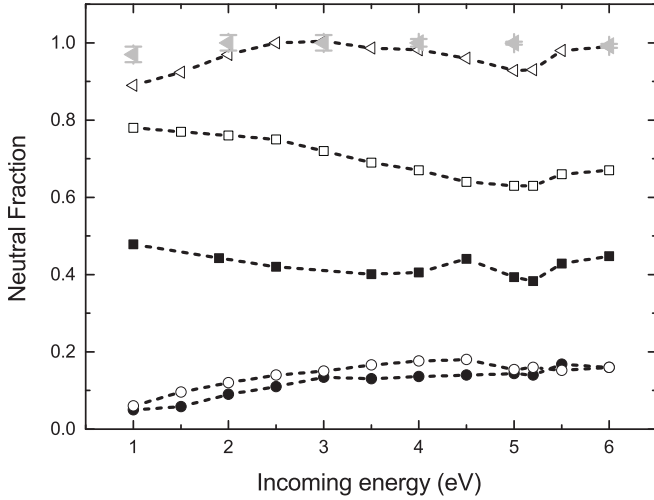


FIG. 2. Neutral fraction as a function of the ion incoming energy. The contribution of the $1s^2$ fundamental state (open squares), the $1s2s$ (full circles), and $1s2p$ (open circles) excited states are differentiated. The total neutral fraction (the sum of the previous three contributions) is represented by open triangles and compared with experimental values (gray full triangles). For contrast purposes, the calculation that only considers neutralization to the fundamental state is shown (full squares).

HOPG surface, with the geometric configuration consistent with the assumptions of the theoretical model used.

IV. COMPARISON BETWEEN THEORY AND EXPERIMENT

In Fig. 2, we show the different contributions to the He^+ neutralization provided by the ground and excited states. The

sum of all of them satisfactorily agrees with the observed neutral fraction.

In this figure, the neutral fraction obtained by disregarding, in our calculation, the excited states as possible neutralization channels (solid squares) is also shown. We can see that in this case, the neutral fraction becomes largely underestimated. The correlation effects introduced by the He excited configurations are responsible for the important increase of the ground-state neutralization probability [15].

The Auger neutralization to the ground state is not considered in our calculation; the oscillatory behavior of the neutral fraction with the incident energy found theoretically and not observed experimentally can be a consequence of this fact.

V. AUGER DEEXCITATION: THEORY

A detailed analysis of the energy evolution, along the trajectory, of the He excited states involved in the ion neutralization leads us to think that the Auger deexcitation mechanism may be a source of high-energy electrons. On the other hand, the presence of high-energy electrons has already been observed in He^+ -induced secondary electron emission (SEE) spectra from HOPG [24,25].

The Auger rate for the deexcitation of the He excited states ($S = 0$ and $S = 1$) has been calculated in a previous work for a grazing motion of the ion, assuming a jellium model to describe the metal surface [18]. In this work, the ion-surface distance is large enough as to consider the ion level energy shifted only by the image potential. In our work, the excited configurations with $S_z = 0$ and $S_z = 1$ are populated during the backscattering of helium positive ions by the HOPG surface. As large normal components of ion velocity are involved, the distance of the closest approach to the surface is small. Then it is necessary to take into account the details of the HOPG band structure, the occupation probabilities of the excited configurations, and the level shifts introduced by the short-range interactions.

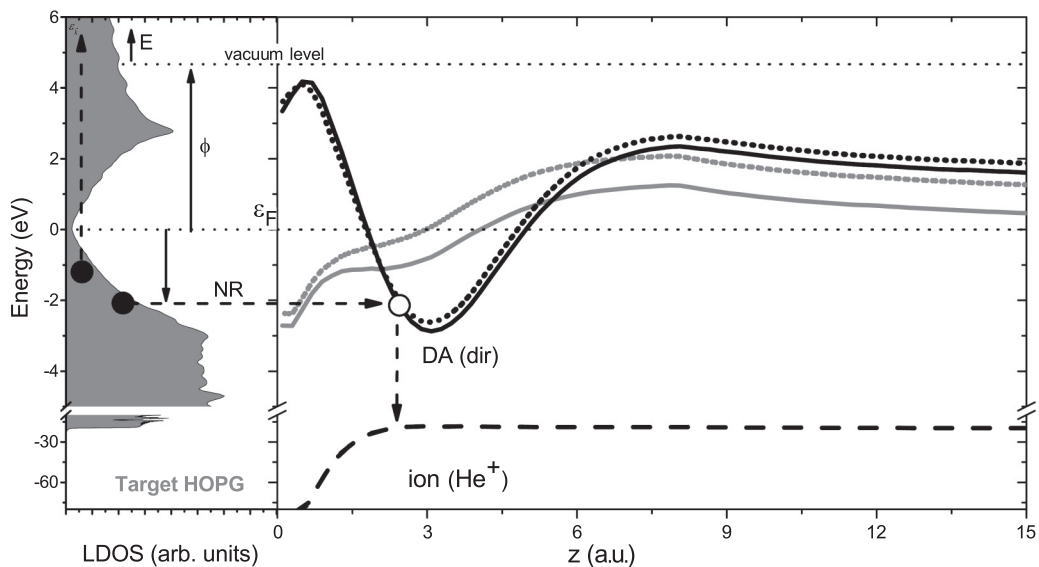


FIG. 3. The one-electron energy levels, defined in Eq. (6), as a function of the distance to the surface. Dashed black line is ε_{1s} , gray solid line is $\varepsilon_{2s,1}$, dashed gray line is $\varepsilon_{2s,0}$, solid black line is $\varepsilon_{2p,1}$, and dotted black line is $\varepsilon_{2p,0}$. In the left panel, the density of states of the HOPG is shown. The zero energy corresponds to the Fermi energy, therefore the kinetic energy of the emitted electrons referring to the vacuum level is $E = \tilde{E} - \phi$, with ϕ being the HOPG work function.

We use the following semiclassical approximation expression for the time derivative of the energy distribution of emitted electrons:

$$\frac{dN(E,t)}{dt} = \sum_{nm,ij,l} \Delta(t) \rho_{nm,ij}(\varepsilon_{1s} - \varepsilon_l + E) \langle n_l(t) \rangle \times f_{<}(\varepsilon_{1s} - \varepsilon_l + E). \quad (5)$$

In Eq. (5), $\rho_{nm,ij}(\varepsilon)$ are the elements of the density matrix of the solid target (nm are orbital indexes; ij are site indexes), $\langle n_l(t) \rangle$ is the time-dependent occupation probability of the excited atom configurations, and $f_{<}(\varepsilon)$ is the Fermi function. The energy $\varepsilon_{\bar{k}}$ of the occupied band state of the solid at which $\rho_{nm,ij}$ and $f_{<}$ are evaluated is determined by the energy conservation requirement,

$$\varepsilon_l + \varepsilon_{\bar{k}} = \varepsilon_{1s} + E.$$

The final energy of the emitted electron is E ; the one-electron energies $\varepsilon_{1s}, \varepsilon_l$, corresponding to the ground and excited states, respectively, are obtained from the difference between the total energies of the respective electronic configurations in the following manner:

$$\begin{aligned} \varepsilon_{1s} &= E(1s^2) - E(1s\sigma), \\ \varepsilon_{2s,0} &= E(1s\sigma 2s\bar{\sigma}) - E(1s\sigma), \\ \varepsilon_{2s,1(-)} &= E(1s\sigma 2s\sigma) - E(1s\sigma), \\ \varepsilon_{2p,0} &= E(1s\sigma 2p\bar{\sigma}) - E(1s\sigma), \\ \varepsilon_{2p,1(-)} &= E(1s\sigma 2p\sigma) - E(1s\sigma). \end{aligned} \quad (6)$$

In Eq. (5), we have assumed that the transition rate time dependence comes only from the variable position of the ion,

$$|\langle \phi_{\varepsilon_k}(r) \phi_l(r') | 1/|r - r'| | \phi_{1s}(r) \phi_E(r') \rangle|^2 \rho_f(E) \approx \Delta(t).$$

In Fig. 3, we can observe the distance variation of the one-electron energies ε_l along the trajectory of the projectile calculated in Ref. [15], contrasted with the density of states of the HOPG [31,32], and in a schematized way the direct Auger deexcitation process (DA) after the resonant neutralization (RN).

Here we only consider the direct Auger deexcitation, i.e., the emission of one surface electron by the decaying process in the atom. This mechanism is expected to be dominant for atom location not very close to the surface and for distances along the exit trajectory at which the resonant neutralization to the excited states has practically taken place. In Fig. 4, we show the probability of occupation for the different states as a function of the distance to the surface along the outgoing trajectory of the projectile. We consider that the Auger deexcitation process is habituated at a characteristic distance z_0 at which the neutralization by the resonant mechanism is already significant and has achieved a practically constant value. By following this criterion, we see in Fig. 4 that z_0 decreases as the projectile energy increases ($z_0 = 2.6, 1.8, 1.7, 1.7$ and 1.6 a.u. for incoming energies of 1, 2, 3, 4, and 5 keV, respectively).

Then, by integrating Eq. (5) from z_0 , we obtain

$$N(E) = \int_{z_0}^{\infty} \frac{dz}{v} \sum_{nm,ij,l} \Delta(z) \rho_{nm,ij}(\varepsilon_{1s} - \varepsilon_l + E) \times \langle n_l(t) \rangle f_{<}(\varepsilon_{1s} - \varepsilon_l + E).$$

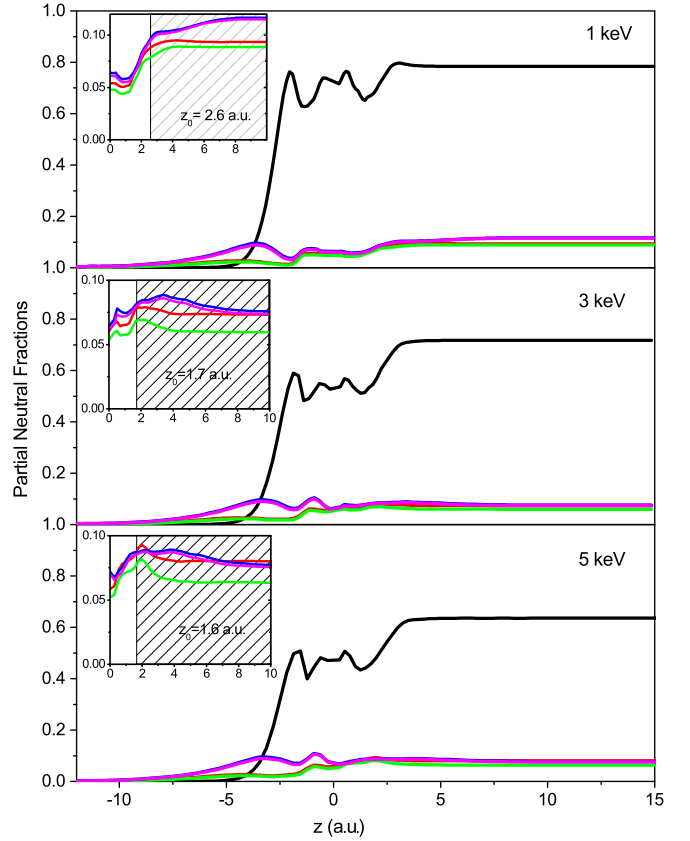


FIG. 4. (Color online) Probability of occupation of the different He electronic configurations as a function of the projectile-surface distance z and for various He^+ incoming energies. Black (upper line at $z = 15$ a.u. in main plots), red (third line from top to bottom at $z = 0$ a.u. in insets), green (fourth line from top to bottom at $z = 0$ a.u. in insets), blue (upper line in insets at $z = 0$ a.u.), and magenta (second line in insets from top to bottom at $z = 0$ a.u.) solid lines correspond to n_{He^0} , $n_{He^0(1s2s, S_z=1, -1)}$, $n_{He^0(1s2s, S_z=0)}$, $n_{He^0(1s2p, S_z=1, -1)}$, and $n_{He^0(1s2p, S_z=0)}$, respectively (see text in Sec. II). Negative (positive) distances indicate incoming (outgoing) trajectories. Insets: the contributions of the excited states to the neutral fraction during the outgoing trajectory are zoomed in. The shadowed area indicates the region where Auger deexcitation is expected.

The results for $N(E)E$, shown in Fig. 5, are obtained by assuming $\Delta(z)$ as an exponentially decaying function given by $\exp[-(z - z_0)/2]$. This is not a completely justified assumption but it is not a key factor in our model; the use of other z dependences, for instance $\Delta(z) = \text{const}$ or the asymptotic behavior $1/z^3$ calculated by using a linear response theory in the case of helium moving parallel to an aluminum surface [18], do not change the physics of our conclusions.

We see from Fig. 5 that the emitted electron spectra show energetic electrons ($E > 15$ eV) that become more important for larger incoming energies of helium ions. These more energetic electrons mainly come from the deexcitation of excited states at distances close to the surface, as can be seen in Fig. 6. The results shown in Fig. 6 are straightforwardly understood by considering the energy-level variations shown in Fig. 3 and the occupation probabilities shown in Fig. 4.

From Fig. 6, we can see that the excited $1s2s$ and $1s2p$ states have a finite probability of occupation in the region closest to

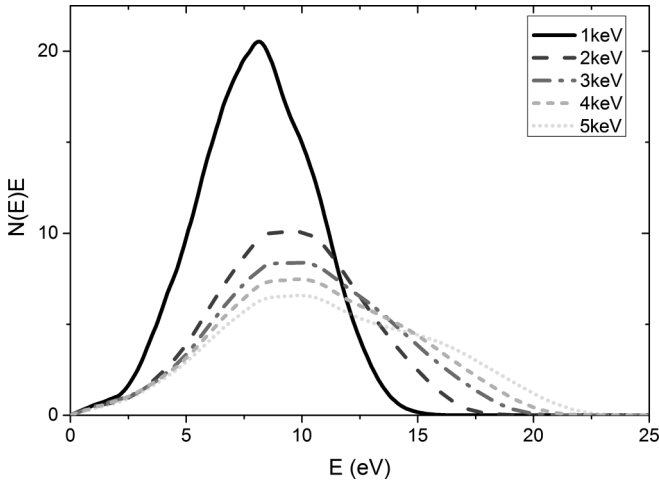


FIG. 5. The emitted electron spectra as a function of the electron energy for several values of the ion bombardment kinetic energy: 1, 2, 3, 4, and 5 keV.

the surface and the energy difference with the ground state is the largest. Therefore, the highest-energy emitted electrons come from this region. The intensity of this electron emission is strongly modulated by the HOPG local density of states close to the Fermi energy.

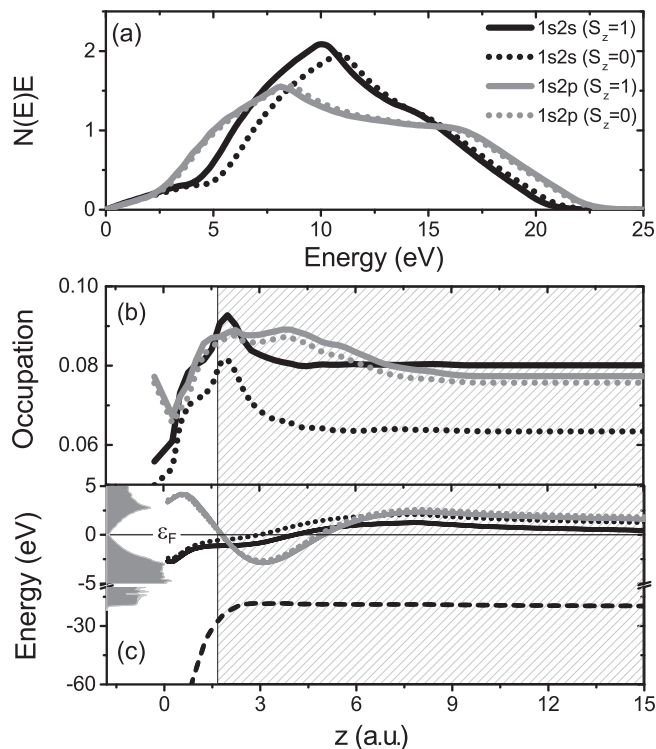


FIG. 6. (a) Contributions to the energy distribution of emitted electrons from the different excited states for an ion bombardment energy of 5 keV. (b) Occupation probability of the excited states along the ion exit trajectory. (c) One-electron energy levels corresponding to the excited states and also to the ground state (black dashed line); the local density of states of the HOPG surface is also shown in this panel. Gray lines correspond to the $1s2p$ excited states and black lines correspond to $1s2s$.

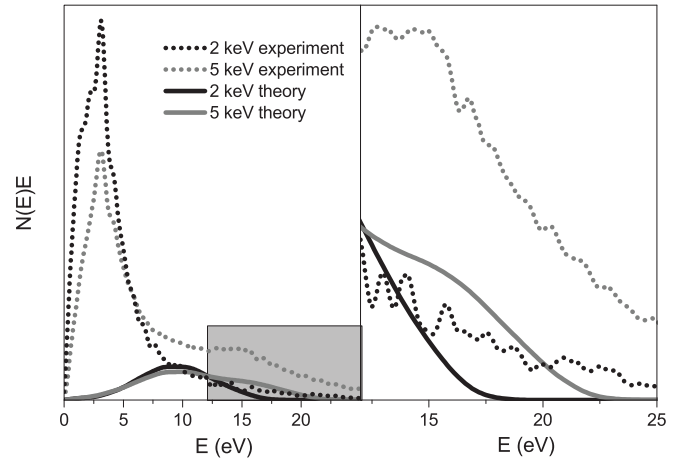


FIG. 7. The emitted electron spectra as a function of the electron energy. Left panel: The measured and calculated spectra for 2 and 5 keV ion incoming energies. Right panel: The high-energy region is zoomed in.

In Fig. 7, we compare experimental spectra with calculated spectra for two different He^+ incoming energies (2 and 5 keV). Experimental spectra were obtained using a hemispherical analyzer and measured spectra were published recently [25].

The true secondary electrons in the experimental spectra ($E < 7$ eV) are mainly related to the electron cascade and Auger neutralization processes, while the electrons emitted with larger energies can be caused by other multiple processes originated in the ion-surface collision: deexcitation of excitons [24], pair electron-hole excitation, and the Auger decaying mechanism of excited states of helium as proposed in the current work. The calculated spectra only involve the energy distribution of electrons generated by the Auger decay of the excited states populated during the ion-surface collision. They show an incoming ion energy dependence typical of Auger processes for low-energy emitted electrons ($E < 15$ eV), but we can see that this deexcitation process also contributes to the tail of energetic emitted electrons and with the same ion energy dependence of the experiment, i.e., the tail becomes more prominent as the ion energy increases (right panel of Fig. 7).

VI. CONCLUSIONS

We present systematic measurements of the neutral fraction of He^+ backscattered from a HOPG surface, proving that a practically full He^+ neutralization occurs in a broad range of incoming energies (1–8 keV). One of the goals of the present work was to confirm experimentally that the first excited configurations of the He atom are necessary to reproduce the experimental results. The agreement with the experiment supports our important conclusion about the relevance of the correlation effects introduced by the first excited states of He, which has also been observed in the scattering of He^+ by an aluminum surface [11]. The other goal of our work was the energy distribution of electrons emitted by Auger deexcitation of the populated excited states of helium, which can be calculated within a semiclassical approximation and consistently with the neutral fraction calculation. We conclude that since the excited states of the He atom are populated during

the collision, the Auger deexcitation mechanism provides a source of emitted electrons in the energy range between 0 and 25 eV. The electrons emitted with energy values larger than 15 eV show an impinging ion energy dependence consistent with experimental results.

ACKNOWLEDGMENTS

This work was supported by ANPCyT (PICT 2010-0294), CONICET (PIP 2012-2014 577 and PIP 2012-2014 621 grants) and U.N.L. (CAI + D 2011 501 201101 00283 LI and CAI + D 2011 501 201101 00180 LI).

-
- [1] H. D. Hagstrum, *Phys. Rev.* **96**, 336 (1954).
[2] R. Brako and D. M. News, *Surf. Sci.* **108**, 253 (1981).
[3] M. Aono and R. Souda, *Nucl. Instrum. Methods Phys. Res., Sect. B* **27**, 55 (1987).
[4] J. Los and J. J. C. Geerlings, *Phys. Rep.* **190**, 133 (1990).
[5] J. B. Marston, D. R. Andersson, E. R. Behringer, B. H. Cooper, C. A. DiRubio, G. A. Kimmel, and C. Richardson, *Phys. Rev. B* **48**, 7809 (1993).
[6] A. G. Borisov, J. P. Gauyacq, E. V. Chulkov, V. M. Silkin, and P. M. Echenique, *Phys. Rev. B* **65**, 235434 (2002).
[7] J. W. Rabalais, *Principles and Applications of Ion Scattering Spectrometry: Surface Chemical and Structural Analysis* (Wiley, New York, 2003).
[8] J. A. Yarmoff, Y. Yang, G. F. Liu, X. Chen, and Z. Sroubek, *Vacuum* **73**, 25 (2004).
[9] A. R. Canário, A. G. Borisov, J. P. Gauyacq, and V. A. Esaulov, *Phys. Rev. B* **71**, 121401 (2005).
[10] E. C. Goldberg, F. Flores, and R. C. Monreal, *Phys. Rev. B* **71**, 035112 (2005).
[11] N. Bajales, J. Ferrón, and E. C. Goldberg, *Phys. Rev. B* **76**, 245431 (2007).
[12] H. H. Brongersma, M. Draxler, M. de Ridder, and P. Bauer, *Surf. Sci. Rep.* **62**, 63 (2007).
[13] A. Gross, *Theoretical Surface Science: A Microscopic Perspective* (Springer-Verlag, Berlin, 2009).
[14] G. G. Andersson, in *Reference Module in Chemistry, Molecular Sciences and Chemical Engineering*, edited by Jan Reedijk (Elsevier, Amsterdam, 2013).
[15] A. Iglesias-García, E. A. García, and E. C. Goldberg, *Phys. Rev. B* **87**, 075434 (2013).
[16] M. L. E. Oliphant and P. B. Moon, *Proc. R. Soc. London A* **127**, 388 (1930).
[17] M. Alducin, F. J. García de Abajo, and P. M. Echenique, *Phys. Rev. B* **49**, 14589 (1994).
[18] M. Alducin, *Phys. Rev. A* **53**, 4222 (1996).
[19] N. Lorente, M. A. Cazalilla, J. P. Gauyacq, D. Teillet-Billy, and P. M. Echenique, *Surf. Sci.* **411**, L888 (1998).
[20] S. N. Mikhailov, L. C. A. van den Oetelaar, and H. H. Brongersma, *Nucl. Instrum. Methods Phys. Res., Sect. B* **93**, 210 (1994).
[21] L. C. A. van den Oetelaar, S. N. Mikhailov, and H. H. Brongersma, *Nucl. Instrum. Methods Phys. Res., Sect. B* **85**, 420 (1994).
[22] R. Souda and K. Yamamoto, *Nucl. Instrum. Methods Phys. Res., Sect. B* **125**, 256 (1997).
[23] N. B. Luna, F. J. Bonetto, R. A. Vidal, E. C. Goldberg, and J. Ferrón, *J. Mol. Catal. A: Chem.* **281**, 237 (2008).
[24] N. Bajales, L. Cristina, S. Mendoza, R. A. Baragiola, E. C. Goldberg, and J. Ferrón, *Phys. Rev. Lett.* **100**, 227604 (2008).
[25] J. Ferrón, R. A. Vidal, N. Bajales, L. Cristina, and R. A. Baragiola, *Surf. Sci.* **622**, 83 (2014).
[26] O. Grizzi, M. Shi, H. Bu, and J. W. Rabalais, *Rev. Sci. Instrum.* **61**, 740 (1990).
[27] P. W. Anderson, *Phys. Rev.* **124**, 41 (1961).
[28] S. Huzinaga, J. Andzelm, M. Klobukowsky, E. Radzio-Andzelm, Y. Sakai, and H. Tatewaki, *Gaussian Basis Set for Molecular Calculations* (Elsevier, Amsterdam, 1984).
[29] S. Huzinaga, *J. Chem. Phys.* **42**, 1293 (1965).
[30] A. A. Radzig and B. M. Smirnov, *Reference Data on Atoms, Molecules, and Ions* (Springer-Verlag, Berlin, 1985).
[31] J. P. Lewis, K. R. Glaesemann, G. A. Voth, J. Fritsch, A. A. Demkov, J. Ortega, and O. F. Sankey, *Phys. Rev. B* **64**, 195103 (2001).
[32] P. Jelinek, H. Wang, J. P. Lewis, O. F. Sankey, and J. Ortega, *Phys. Rev. B* **71**, 235101 (2005).